A TEST OF GLOBAL CONTRACTION MODELS FOR MARS USING OBSERVATIONS.

Amanda L. Nahm[1] and Richard A. Schultz[1] [1]Geomechanics–Rock Fracture Group, Department of Geological Sciences and Engineering/172, University of Nevada, Reno, NV 89557–0138, nahma@mines.unr.edu

Summary: Faults provide a record of a planet's crustal stress state and interior dynamics, including volumetric changes related to long-term cooling. Previous work has suggested that Mars experienced a pulse of large-scale global contraction during Hesperian time (3.1 Ga to 3.6 Ga). Here we evaluate the evidence for Martian global contraction using a recent compilation of both normal and thrust faults and show that, when fault-related strains are calculated, there is no evidence for a significant episode of compressional deformation from global contraction on Mars. In addition, when these values of fault-related strain are compared to the surface strain predicted by thermal models, we find that the amount of global contraction predicted by thermal models is larger than what is recorded by the faults at the surface.

Introduction: Mars has a complex geologic and tectonic history. Nearly 15,000 faults have been mapped globally [1] in all ages of rocks. A peak in volcanic eruptions has been suggested in the Early Hesperian (3.1 Ga to 3.6 Ga [2]), which has been linked to the formation of the extensive Hesperian ridged plains [3]. Rapid cooling of Mars may have resulted from the global effusion of lava, contributing to global contraction, which led to compressional tectonism at the surface [4]. A concentration of contractional structures occurs in the Early Hesperian across Mars [4,5], leading to the postulate that these structures had a single global origin [3, 4, 6-8]. The hypothesis that wrinkle ridges [9] and lobate scarps formed by global contraction [3,4, 8, 10], or decrease in planetary radius, is tested here for the first time by calculating the horizontal crustal strain accommodated by the faults and converting it into planetary radius change, permitting a quantitative comparison between fault-related strain and strain predicted by models of the thermal evolution of Mars.

Previous tectonic models: The distribution of wrinkle ridges across the planet is uneven (Fig. 1, blue faults), with ridges being confined primarily to volcanic ridged plains units of Lower Hesperian age (3.1–3.6 Ga [2]), suggesting that ridge formation may have been concentrated during that time (3, 4, 6, 7]. The largest concentration of contractional structures on Mars is located in the ridged plains surrounding Tharsis in the western hemisphere and is oriented approximately circumferentially to the proposed center of activity [3, 4, 7, 11]. However, secondary concentrations of wrinkle ridges and lobate scarps are not circumferential to Tharsis and are found in both the eastern and western hemispheres (Fig. 1), including Lunae and Solis Plana, Memnonia, Noachis Terra, Hesperia Planum, Terra Cimmeria, Syrtis Major, Arabia Terra, and Elysium Planitia [4] perhaps suggesting multiple regional and/or global mechanisms.

Thermal history models: Patterns of global tectonic deformation on a planetary surface can be used as evidence of the global thermal evolution of the body [3, 12, 13]. For a planet with a one-plate lithosphere, such as Mars or Mercury, temperature changes in its interior can result in changes in its surface area [3]. For a cooling interior, horizontal contractional strain would accumulate in the lithosphere, and could create contractional faults, such as lobate scarps and wrinkle ridges [3]. Like Venus and Earth, the thermal history of Mars is that of secular cooling [3], so evidence of global contraction in the form of contractional faults should be observable at the surface as previous workers have inferred from qualitative grounds.

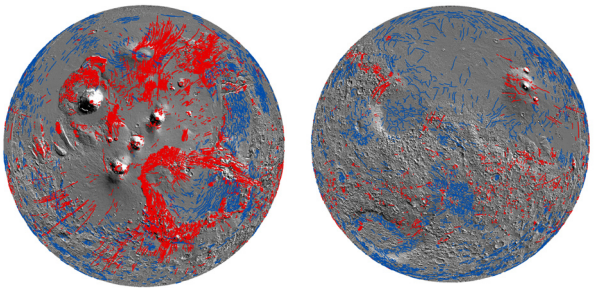

Figure 1. Global distribution of faults on Mars. Red: Extensional faults, Blue: Contractional faults. Western hemisphere, left and eastern hemisphere, right. Data and figure courtesy of M. Knapmeyer, DLR and M. Weller, UNR.

Methods: Faults mapped by [1, 5] were used in this study. These normal and thrust faults were mapped on 1 km/pixel Mars Orbiter Laser Altimeter (MOLA) digital elevation models and assigned maximum ages based on crater retention ages of the global 1:15,000,000 scale geologic maps of Mars [1, 5, 14-16]. [1, 5] do not distinguish between thrust faults and wrinkle ridges, so both end-member cases are used here.

The strain and corresponding planetary radius change associated with faults scale with the amount of contraction or extension across them (the fault displacement, D). We calculate horizontal normal strain and radius change using displacement-length (D/L) scaling, as has been done in previous studies for Mars and Mercury. Typical D/L ratios (γ) for normal faults, surface-breaking thrust faults, and wrinkle ridges were used to calculate the total horizontal normal strain for each set of fault ages (i.e. Noachian, Hesperian, etc.). Fault lengths of both normal and thrust faults were considered for two time intervals: Middle Noachian to Late Amazonian (0 – 4.0 Ga [2]), corresponding to the cumulative global cooling-related strain, and Late Noachian to Early Hesperian (3.4 –3.8 Ga [2]), corresponding to the "Early Hesperian pulse". Strain and corresponding radius change values were calculated for both an average thickness of the Martian lithosphere of T = 30 km [5] and T = 40 km. Fault lengths (L), fault dip (δ), D/L ratio (γ), and volume of the deformed layer ($V = (4/3)\,\pi\,[R_p^3 - (R_p^3 - T)]^3$ (1)) were used in Kostrov's formula, $\varepsilon_n = [(\gamma \sin\delta \cos\delta)/2V]\,\Sigma L^3$ (2) [17], to determine the total strain accommodated by the faults for all 4 cases (Table 1). Dip angles considered are 60° for normal faults and 30° for the thrust faults beneath wrinkle ridges and lobate scarps. The deformed volume was calculated by using depths of faulting T obtained from mechanical modeling of the structural topography. The values of strain were used to calculate the change in radius using $\Delta R = R_p - \sqrt{[R_p^2/(\varepsilon_n + 1)]}$ (3), where ΔR is

the change in the Martian radius, R_p is the current radius (3397 km), and ε_n is the horizontal normal strain [18]. Values for the net radius change were calculated by subtracting the radius decrease (from contraction) from the radius increase (from extension) (Table 1). Calculated values for strain and radius change for $T = 40$ km are not shown and are 33% larger (more positive or negative) than values for $T = 30$ km.

	% Strain (ε_n)	Radius change (m)	Net radius change (m)
Normal faults, MN-LA	0.0879	1492.0	1176.8
Wrinkle ridges, MN-LA	-0.0186	-315.2	
Normal faults, LN-EH	0.00561	95.3	32.8
Wrinkle ridges, LN-EH	-0.00368	-62.5	
Normal faults, MN-LA	0.0879	1492.0	861.5
Lobate scarps, MN-LA	-0.0371	-630.5	
Normal faults, LN-EH	0.00561	95.3	-29.8
Lobate scarps, LN-EH	-0.00736	-125.1	

Table 1. Results of the strain and radius change calculations for $T = 30$ km. Negative values, contractional strain and radius decrease; Positive values, extensional strain and radius increase. MN: Middle Noachian; LN: Late Noachian; EH: Early Hesperian; LA: Late Amazonian; ε_n horizontal normal strain.

To compare the observable strain recorded by the surface faults to the values of strain predicted by thermal models, we subtracted the calculated values of strain (only for thrust faults or wrinkle ridges) for the Hesperian-aged faults and for faults of all ages (Table 1) from calculated values of total contractional strain [13] for two thermal models (W&D [19], L&F [20]) for both time intervals considered. These values of strain were converted to values of radius change by using equation (3).

Results: We find that Martian radius decreases occur for only 1 of 4 cases (Table 1), which requires the compressional structures to all be lobate scarps, rather than the lower-strain wrinkle ridges, in conflict with observations [21]. A radius decrease of only ~30 m occurs during the Late Noachian to Early Hesperian, for which the pulse of global contraction has been hypothesized based on the observed concentration of contractional faults in rocks of this age. Assuming only contractional faults, radius decreases range from 62.5 m to 630 m for $T = 30$ km and $\delta = 30°$ (Table 1). However, since extensional faults also formed during these times, resulting in a corresponding average increase of the planet's radius, these faults cannot be neglected, and the net radius change is more representative of the total fault-related strains.

In all cases, comparisons of the observed fault-related strain with strains predicted by the thermal models show that the thermal models predict substantially more strain than is recorded by the faults. For both thermal models, the radius decrease is over-predicted by ~1 km for both wrinkle ridges and lobate scarps during the Hesperian; the values for 'missing' global contraction for all of Mars' history are similar to these values (~1.2 km and ~1 km for wrinkle ridges and lobate scarps, respectively).

	Model	Hesperian	MN–LA
Strain ratio	W&D/WR	14.9	15.6
	W&D/LS	6.5	6.8
	L&F/WR	15.2	16.7
	L&F/LS	7.6	8.3
ΔR (m)	W&D - WR	1011	1156
	W&D - LS	939	1077
	L&F - WR	1031	1238
	L&F - LS	959	1159

Table 2. Comparison between fault-related strain and strain predicted by the thermal models and corresponding radius change. W&D: Wänke and Dreibus, (1994) model [19]; L&F: Lodders and Fegley, (1997) model [20]; WR: strain from wrinkle ridges; LS: strain from lobate scarps; MN: Middle Noachian, LA; Late Amazonian; Strain ratio: ratio of predicted thermal strain to fault-related strain; ΔR: calculated change in radius [18] based on the difference between predicted thermal strain and fault-related strain for both models (W&D and L&F) and lobate scarps and wrinkle ridges. Values show the amount of strain or radius change over-predicted by the thermal models.

Conclusions: The results show that the cumulative contractional strains at the Martian surface predicted by thermal history models exceed those recorded by contractional structures by a factor of ~7.5 (assuming all structures are wrinkle ridges) or ~3.5 (assuming all are lobate scarps). We also find no evidence for a "pulse" of enhanced contractional strain during the Hesperian as has been previously hypothesized. The observations of contractional deformation support a smaller degree of strain and radius change than thermal history models of Mars currently predict.

References: [1] Knapmeyer, M., *et al*. (2008) EGU abstract 2008–A–03574. [2] Hartmann, W. K., and Neukum, G. (2001) *Space Sci. Rev.*, **96**, 165–194. [3] Schubert, G. *et al.*, (1992) *Mars*, 147–182. [4] Watters, T. R. (1993) *J. Geophys. Res.*, **98**, 17,409–17,060. [5] Knapmeyer, M., *et al*. (2006) *J. Geophys. Res.*, **111**, 10.1029/2006JE002708. [6] Watters, T. R. and Maxwell, T. A., (1983) *Icarus*, **56**, 278–298. [7] Watters, T. R. and Maxwell, T. A., (1986) *J. Geophys. Res.*, **91**, 8113–8125. [8] Mangold, N. *et al.*, (2000) *Planet. Space Sci.*, **48**, 1201–1211. [9] Schultz, R. A., (2000) *J. Geophys. Res.*, **105**, 12,035–12,052. [10] Phillips, R. J., (1991) LPI Tech. Rep. 91-02 LPI/TR-91-02, Lunar and Planetary Institute, Houston, 35–38. [11] Wise, D. U. *et al.*, (1979) *Icarus*, **38**, 458–472. [12] Banerdt *et al.*, (1992) *Mars*, University of Arizona Press, 240–297. [13] Andrews-Hanna, J. C. *et al.*, (2008) *J. Geophys. Res.*, **113**, E08002, 10.1029/2007JE002980. [14] Scott, D. H. *et al.*, (1986) USGS Misc. Inv. Series Map, I–802–A. [15] Scott, D. H. *et al.*, (1987) USGS Misc. Inv. Series Map, I–1802–B. [16] Scott, D. H. *et al.*, (1987) USGS Misc. Inv. Series Map, I–1802–C. [17] Scholz, C. H., (1997) *Geowissenschaften*, **15**, 124–130. [18] Watters, T. R. *et al.*, (2009) *Planetary Tectonics*, Cambridge University Press. [19] Wänke, H. and Dreibus, G., (1994) *Phil. Trans. R. Soc. Lond.*, **349**, 285–293. [20] Lodders, K. and Fegley Jr., B., (1997) *Icarus*, **126**, 373–394. [21] Tanaka, K. L. et al., (1991) *J. Geophys. Res.*, **96**, 15617–15633.

Abstract published in Lunar and Planetary Science *XLI*, CD-ROM (www.lpi.usra.edu/meetings), Lunar and Planetary Institute, Houston (2010).